



Energy distribution and effective components analysis of 2^n sequence pseudo-random signal

Yang YANG¹, Ji-shan HE^{2,3}, Di-quan LI³

1. Geotechnical and Structural Engineering Research Center, Shandong University, Ji'nan 250061, China;
2. Institute of Urban Underground Space and Energy Studies,
Chinese University of Hongkong, Shenzhen 518172, China;
3. School of Geosciences and Info-Physics, Central South University, Changsha 410083, China

Received 2 March 2021; accepted 29 June 2021

Abstract: In order to extract usable harmonics from real 2^n sequence pseudo-random data, a technical method is proposed. An equation for predicting the average amplitude of the main frequencies is proposed to guide the choice of signal type for different exploration tasks. By the threshold of the amplitude of the transmitted signal, a set of candidate frequencies are first selected. Then, by operating a spectrum envelope method at these candidate frequencies on received data, effective components in data are extracted. A frequency density calculation method is proposed based on a logical number summation method, to reasonably characterize the frequency density in different frequency bands. By applying this method to real data in Sichuan, China, with signal Type 13, 75 effective components are extracted, including both main frequencies and harmonics. The result suggests that the number of effective frequencies in the 2^n sequence pseudo-random signal can be increased by extracting usable harmonics, without any additional fieldwork.

Key words: electromagnetic prospecting; 2^n pseudo-random signal; energy conservation; harmonic extraction; frequency density

1 Introduction

The frequency-domain controlled-source electromagnetic (CSEM) method has been widely used in mineral resources, geological hazard exploration, and oil-gas exploration [1–4]. In frequency-domain electromagnetic (EM) exploration, the response of ground is embedded in the received signal, and different frequencies involve different electromagnetic energy diffusion characters. By applying certain geophysical inverse algorithms, it is possible to obtain detailed geophysical information about the subsurface. This is the basis for the frequency-domain EM method.

A periodic square wave is frequently used as the transmitter waveform for EM exploration.

Compared with a sine wave, the square wave is easier to implement in hardware, especially when a large current is needed. For the periodic square wave, most of the transmitted energy is distributed on the main frequency, and at most time only one frequency is obtained at one time, which makes it not quite convenient for frequency-domain EM exploration, especially in those high-cost areas. More efficient waveforms are needed. In the field of radar communications, a variety of waveforms are designed to meet the needs of different situations [5–8]. However, due to the different principles of communication and geophysical prospecting, many methods are not suitable for geophysical prospecting signals designing. According to the characteristics of geophysical methods, many waveforms based on different

Corresponding author: Ji-shan HE, Tel: +86-731-88877075, E-mail: hejishan@csu.edu.cn

DOI: 10.1016/S1003-6326(21)65641-8

1003-6326/© 2021 The Nonferrous Metals Society of China. Published by Elsevier Ltd & Science Press

methods are designed and created for different geophysical purposes, in which energy is distributed at more frequencies, such as binary symmetric waveform by an analytical method [9], pseudo-random binary sequence (PRBS) [10], and specialized waveforms for CSEM [11–13]. All these waveforms have quite good spectrum properties. In these signals, it is not necessary to continuously change the sending frequency. But it still needs to be changed especially when there are a lot of frequencies of interest. 2^n sequence pseudo-random signal was developed to design more adaptive and complicated waveforms to obtain more desired frequencies [14–16]. The 2^n sequence pseudo-random signal is formed by the self-closed addition of $-1, 0, 1$ three elements and its main frequencies are distributed according to 2^n . It is a multi-frequency pseudo-random signal with main frequencies that uniformly distributed in the logarithmic frequency coordinates [16], which makes it a quite efficient signal for frequency-domain EM exploration. And recently, high order 2^n pseudo-random sequences have been designed based on traditional 2^n sequence pseudo-random signal [17,18].

In previous researches, only the main frequencies of 2^n pseudo-random signal are used, without attention to the effectiveness of harmonic components [9–11]. In fact, for a pseudo-random signal, especially a 2^n sequence pseudo-random signal, many harmonics are of considerable amplitude, which can be further used for real exploration. If these effective harmonic components are extracted, it will increase the number of frequencies and further improve the exploration result. However, most of the frequency-domain electromagnetic exploration equipments, especially artificial source electromagnetic equipments, traditionally only save quite limited coefficients, rather than complete time series of signal, which makes it not easy to systematically analyze the spectrum of the prospecting signal and extract the effective harmonic components.

Since data storage technology and computing capabilities have been greatly developed, more and more electromagnetic equipments can record and save complete time-series signals on a large scale. For example, the wide field electromagnetic method (WFEM) using 2^n sequence pseudo-random signals has made the rapid storage of large-scale and

high-sampling rate data possible since 2013, including both the current data and received data, which provides a prerequisite for full-frequency data analysis and harmonic extraction.

In this work, we first simulated the 2^n sequence pseudo-random ideal signal with different types and systematically analyzed the spectrum characteristics for different 2^n sequence pseudo-random signal. Based on the law of energy conservation, we proposed an equation to predict the average amplitude of the main frequencies in the 2^n sequence of a pseudo-random signal. After that, we filtered the main frequencies and some harmonics with different amplitude thresholds to obtain potential effective frequencies. Finally, a real case was involved to illustrate the extraction for qualified frequencies as effective components based on a spectrum envelope method. We also proposed an algorithm calculation of frequency density to obtain the distribution characteristics of those effective components, making the extraction results more instructive.

2 Energy distribution characteristics of 2^n sequence pseudo-random signal

2.1 Energy conservation in time domain and frequency-domain

The waveform and spectrum of the 2^n sequence pseudo-random of Type 7-2 are shown in Fig. 1, in which there are 7 main frequencies from 1 to 64 Hz. Its amplitude in time domain is 100 A. For the 2^n sequence pseudo-random signal with an odd n , there exist only $+100$ A and -100 A in the waveform, and no zero value in the time domain [15]. In the frequency-domain, the average amplitude of the main frequencies is 44.25 A. It is obvious that there are quite a lot of harmonics with considerable amplitudes, such as the amplitude of 17 Hz greater than 20 A. If we add the amplitudes of different frequencies together, it is far larger than 100 A. In fact, the energy of any signal is conserved in both the frequency-domain and the time domain. In this work, we proceed from the Parseval Identity to show the energy conservation of 2^n sequence signals in the time domain and frequency-domain.

2.1.1 Different forms of Fourier series

Assuming the transmitted signal $f(t)$ has a period of 1, $f(t)=f(t+1)$, $f(t)$ can then be expressed through the sine wave with the frequency of 1 Hz

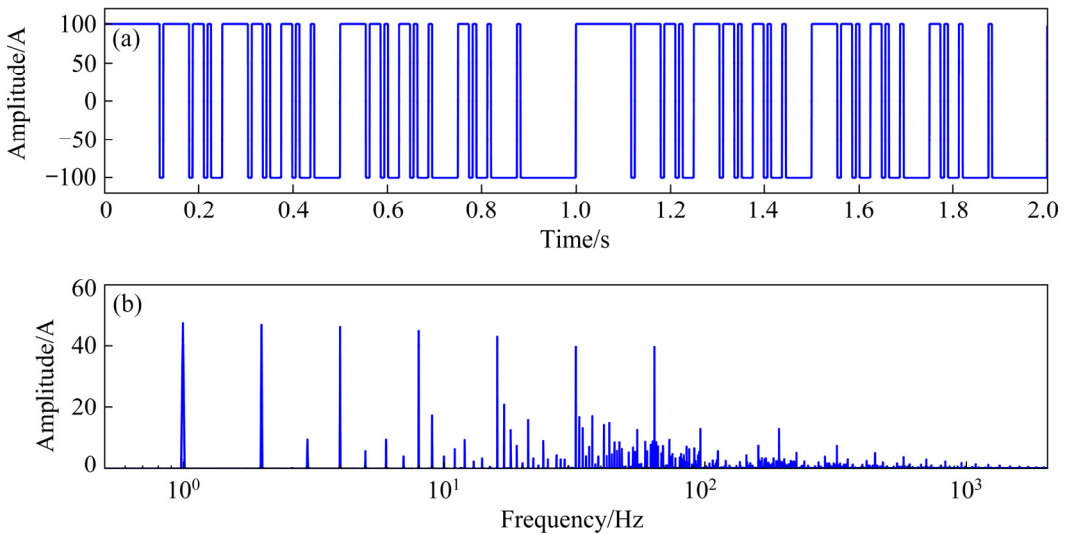


Fig. 1 Waveform (a) and spectrum (b) of 2^n pseudorandom signal in Type 7-2

and its harmonics:

$$f(t) = \sum_{n=1}^{\infty} A_n \sin(2\pi nt + \varphi_n) \quad (1)$$

where A_n is the amplitude of different frequency components, and φ_n is the phase.

By introducing the cosine function, $f(t)$ is written as

$$f(t) = \sum_{n=1}^{\infty} (a_n \cos(2\pi nt) + b_n \sin(2\pi nt)) \quad (2)$$

where $|A_n| = \sqrt{a_n^2 + b_n^2}$.

If there is a direct component (DC) that means $n=0$, the series becomes

$$f(t) = \frac{a_0}{2} + \sum_{n=1}^{\infty} (a_n \cos(2\pi nt) + b_n \sin(2\pi nt)) \quad (3)$$

where $a_0/2$ is the DC component. The amplitudes of most exploration signals oscillate positively and negatively at the center point of 0, so the DC component is 0. However, this series form is not convenient for large-scale calculations. Equation (3) needs to be further simplified. As shown in Eq. (4), the sine and cosine functions can be expressed by complex exponential functions according to Euler's equation:

$$\cos(2\pi nt) = \frac{\exp(2\pi int) + \exp(-2\pi int)}{2} \quad (4a)$$

$$\sin(2\pi nt) = \frac{\exp(2\pi int) - \exp(-2\pi int)}{2} \quad (4b)$$

Bringing Eq. (4) into Eq. (2) can simplify the series to obtain a more concise representation of complex exponential series [19]:

$$f(t) = \sum_{n=-\infty}^{\infty} c_n \exp(2\pi int) \quad (5)$$

where c_n is the coefficient of the complex exponential, and the variable n ranges from $-\infty$ to $+\infty$, which is the origin of the concept of positive and negative frequencies in the Fourier transform and series. If $f(t)$ is real then $c_{-n} = \overline{c_n}$, which means that c_n and c_{-n} are complex conjugates, and $|c_n| = 1/2 \sqrt{a_n^2 + b_n^2}$. In Eq. (2), for a real function $f(t)$, $A_n = 2|c_n|$, and A_n is the amplitude of the corresponding sinusoidal function or signal.

2.1.2 Energy conservation based on Parseval identity

The energy conservation of a signal, based on Parseval identity, can be expressed as

$$\int_{-\infty}^{+\infty} |f(t)|^2 dt = \int_{-\infty}^{+\infty} |F(s)|^2 ds \quad (6)$$

where $f(t)$ is the signal in time domain signal and $F(s)$ is the signal in frequency-domain. Essentially, the signal representation in the time domain uses a standard orthogonal basis, while the frequency-domain uses another standard orthogonal basis. The Fourier transform is just a bridge from one domain to another. Although the representation is different, the contained information and energy are equivalent. For continuous functions, the energy is conserved in both frequency and time domains.

In real exploration, the recorded signal is discrete. Discrete Fourier transform is applied to converting discrete time domain data to frequency-domain data [19]:

$$F[m] = \sum_{n=0}^{N-1} f[n] \exp\left(-\frac{2\pi i m n}{N}\right) \quad (7)$$

$$f[n] = \frac{1}{N} \sum_{m=0}^{N-1} F[m] \exp\left(\frac{2\pi i m n}{N}\right) \quad (8)$$

where N is the signal length, for convenience, n starts from 0 instead of $-N/2$, and the periodic property equation of the complex exponential function still holds; m is the index of frequency-domain coefficients; n is the index of time domain coefficients. Equation (9) can be obtained by finding L2 norm on both sides of Eq. (7):

$$\begin{aligned} |F[m]|^2 &= \sum_{n=0}^{N-1} f[n] \exp\left(-\frac{2\pi i m n}{N}\right) \cdot \\ &\quad \sum_{n'=0}^{N-1} f[n'] \exp\left(\frac{2\pi i m n'}{N}\right) \\ |F[m]|^2 &= \sum_{n=0}^{N-1} f[n] \sum_{n'=0}^{N-1} f[n'] \exp\left(-\frac{2\pi i m (n-n')}{N}\right) \\ \sum_{m=0}^{N-1} |F[m]|^2 &= \sum_{m=0}^{N-1} \sum_{n=0}^{N-1} f[n] \cdot \\ &\quad \sum_{n'=0}^{N-1} f[n'] \exp\left(-\frac{2\pi i m (n-n')}{N}\right) \\ \sum_{m=0}^{N-1} |F[m]|^2 &= \sum_{n=0}^{N-1} f[n] \sum_{n'=0}^{N-1} f[n'] \cdot \\ &\quad \sum_{m=0}^{N-1} \exp\left(-\frac{2\pi i m (n-n')}{N}\right) \end{aligned} \quad (9)$$

When $n=n'$,

$$\sum_{m=0}^{N-1} \exp(-2\pi i m (n-n')/N) = N,$$

and when $n \neq n'$,

$$\sum_{m=0}^{N-1} \exp(-2\pi i m (n-n')/N) = 0,$$

which means that the sum of a complex exponential throughout length N is always equal to zero. The simplification of Eq. (9) is shown as

$$\sum_{m=0}^{N-1} |F[m]|^2 = \sum_{n=0}^{N-1} f[n] \sum_{n'=0}^{N-1} f[n'] \cdot$$

$$\begin{aligned} &\sum_{m=0}^{N-1} \exp\left(-\frac{2\pi i m (n-n')}{N}\right) \\ &\sum_{m=0}^{N-1} |F[m]|^2 = \sum_{n=0}^{N-1} f[n] \sum_{n'=0}^{N-1} f[n'] N \delta_{nn'} \\ &\sum_{m=0}^{N-1} |F[m]|^2 = N \sum_{n=0}^{N-1} f[n] f[n] \\ &\sum_{m=0}^{N-1} |F[m]|^2 = N \sum_{n=0}^{N-1} |f[n]|^2 \end{aligned} \quad (10)$$

Equation (10) is the discrete form of Parseval identity. Note that the value of $F[k]/N$ in Eq. (8) corresponds to the coefficient c_k in the frequency-domain in Eq. (5), and $|c_n|=A_n/2$, which means in the Parseval identity, the coefficients in the frequency-domain is numerically 1/2 of the amplitude A_n of different frequencies. As shown in Eq. (10), the sum of squares of coefficients in the frequency-domain is equal to the sum of squares of amplitudes in the time domain.

The waveform and spectrum of the sine wave and square wave with frequency at 1 Hz and amplitude of 100 A are shown in Fig. 2. It should be noted that to distinguish different spectrums when multiple waveforms are drawn at the same time, we use the Plot command in MATLAB to draw them. Since the data are discrete, the frequency spectrum is a series of polylines. As shown in Fig. 2(b), the sinusoidal signal only has energy at 1 Hz, and there is no data at other frequencies.

The sine wave undergoes complex exponential Fourier transform to obtain the spectrum whose amplitudes of the positive and negative frequencies are 50 A, that is, $|c_k|$ is equal to 50 A, and the sum of $|c_k|$ and $|c_{-k}|$ is 100 A, which means amplitude of 100. The amplitude of the main frequency in the 1 Hz square wave is 127.3 A. In fact, the corresponding amplitude of ± 1 Hz is 63.66 A. The sum of the two results is 127.3 A, which corresponds to A_n in Eq. (1). The energies of the square wave and the sine wave with the same amplitude are not same, and the square wave is significantly larger than the sine wave. There are a lot of harmonic components in the square wave, while the sine wave has no harmonics.

Figure 3 shows the relationship between the energy summation of the square wave in the frequency-domain and the number of harmonics participating in the calculation. As the number of

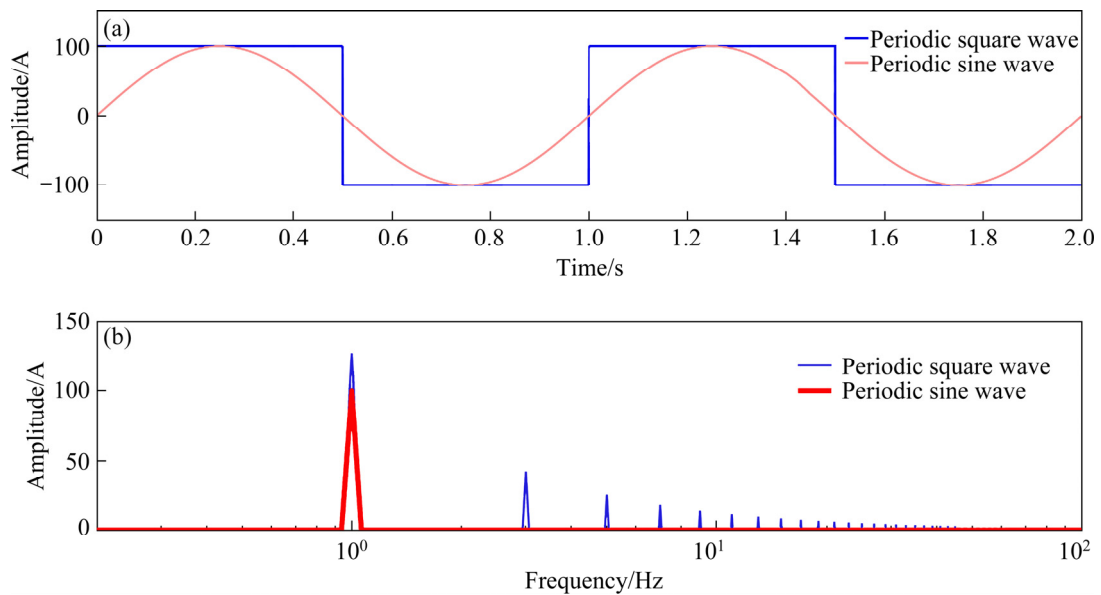


Fig. 2 Waveform (a) and spectrum (b) of 1 Hz periodic sine signal and 1 Hz periodic square wave

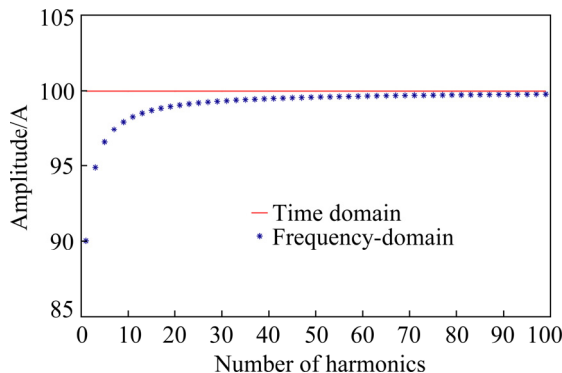


Fig. 3 Energy in time domain and frequency-domain versus number of harmonics

harmonics included in the calculation increases, the amplitude of the frequency-domain gradually approaches a value of 100 A. If we add the sum of the squares of coefficients at all frequencies and perform the square root operation, it is equal to the amplitude of the time domain, which means that the energy is conserved in both time domain and frequency-domain.

2.2 Variation law of main frequencies amplitude

In the 2^n sequence pseudo-random signal, with the number of main frequencies increasing, the energy is evenly distributed on main frequencies, and the amplitude of the main frequencies decreases, as shown in Fig. 4. The amplitude of main frequencies is 127.3 A for 2^n sequence pseudo-random signal in Type 1 (a periodic square wave), and is 72.5 A in Type 3, is 54.1 A in Type 5,

and is 44.3 A in Type 7. As the number of main frequencies increases, the decrease in average amplitude is not linear. The reason is that the energy of a signal is positively related to the square of the amplitude, rather than the amplitude itself.

The odd 2^n sequence pseudo-random signals from Type 1 to Type 19 are sequentially generated according to the self-closed addition operation, and the average amplitude of the main frequencies is respectively calculated, as shown in Fig. 5. The average amplitude is about 33.9 A in Type 11, is about 28.3 A in Type 15, and is about 23.4 A in Type 21. As the number of main frequencies increases, the current amplitude corresponding to the main frequencies does not decrease rapidly. The amplitude of Type 21 is 53% of Type 7 although the number of its main frequencies is 3 times as much as Type 7. If the number of main frequencies continues to increase, the amplitude attenuation becomes much slower. Therefore, according to the calculated results, an approximate equation was proposed to predict the average frequency amplitude in the 2^n sequence pseudo-random signal based on the average amplitude of the main frequencies:

$$y = 0.99\sqrt{127.3^2/x} \exp(-0.01x) \quad (11)$$

where y is the predicted average amplitude, x is the main frequency, 127.3 is the main frequency amplitude corresponding to a periodic square wave with a single frequency amplitude of 100 A, and

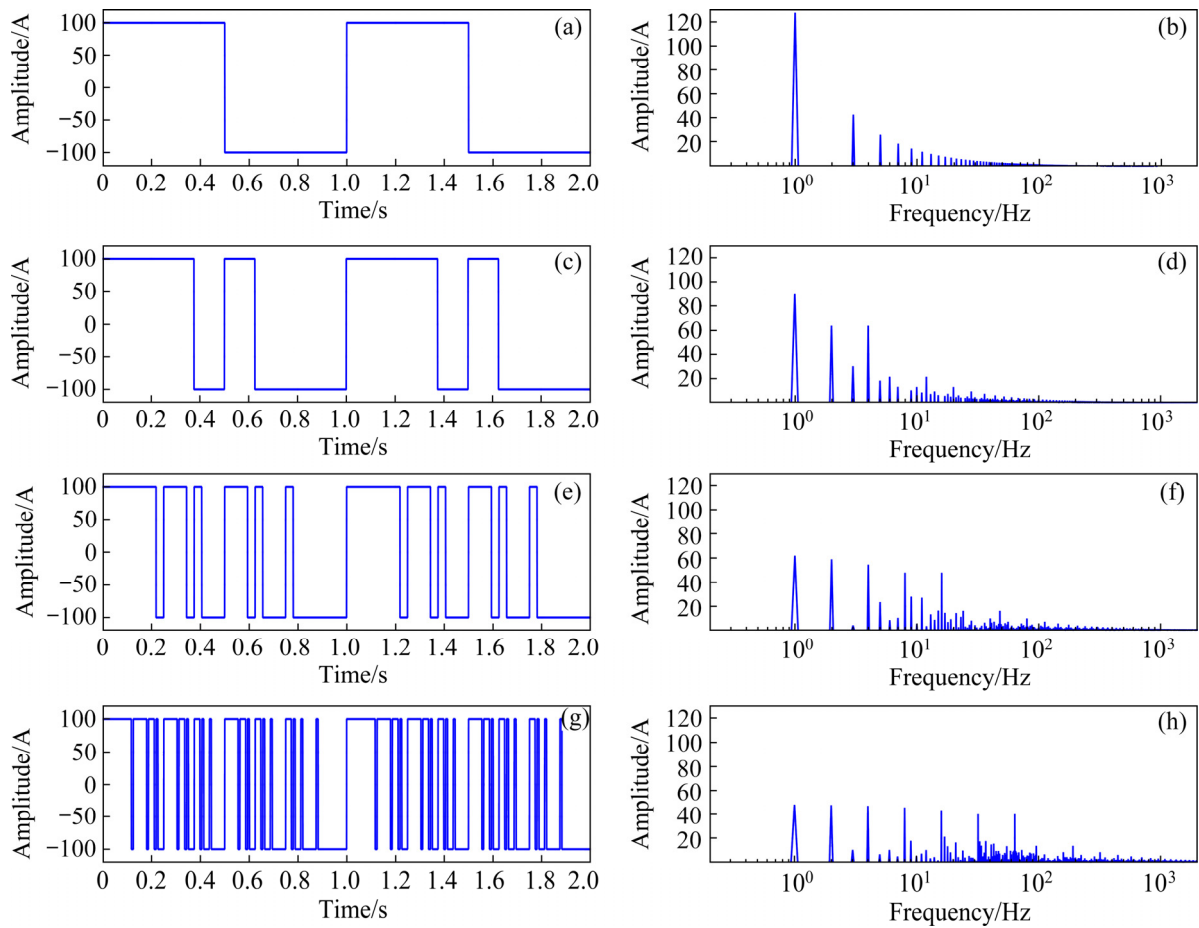


Fig. 4 Waveforms (a, c, e, g) and spectra (b, d, f, h) of 2^n sequence pseudo-random signal in Type 1 (a, b), 3 (c, d), 5 (e, f) and 7 (g, h)

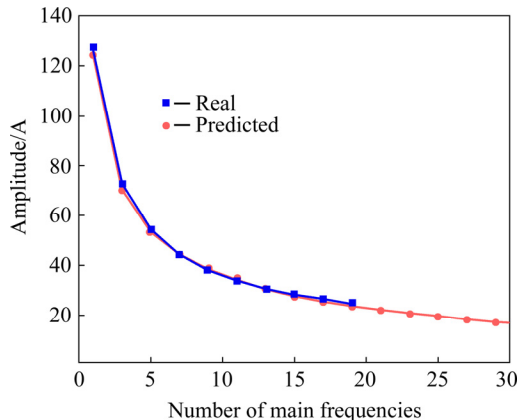


Fig. 5 Comparison of average amplitude prediction curve of main frequencies and real average amplitude of 2^n pseudo-random simulation signal

0.99 and $\exp(-0.01x)$ are the correction coefficients. The physical interpretation of the equation is that if the energy of the main frequencies in 100 A single-frequency periodic square wave is used as standard energy, the energy is proportional to the

sum of squares. x represents the number of halves of the energy, and y represents the amplitude of the energy divided by x . For the 2^n sequence pseudo-random signal, because of its uniform and broad-spectrum characteristics, its energy is also distributed in the harmonics except for the main frequencies, so correction coefficients need to be introduced to make the prediction equation more accurate. As shown in Fig. 5, the amplitude curve calculated according to Eq. (11) can well fit the variation trend of the amplitude of 2^n sequence pseudo-random signal, and it is possible to predict the corresponding average amplitude of signals with more main frequencies. In practical applications, considering the total current of signal emission and the actual situation of external interference, an efficient and reasonable exploration signal type can be generated according to the prediction equation. And high order 2^n sequence pseudo-random signal also follows this equation.

3 Effective components in 2^n sequence pseudo-random signal

3.1 Energy distribution of 2^n sequence pseudo-random simulation signal

The previous analysis shows that the energy of the 2^n sequence pseudo-random signal is mainly distributed at the main frequencies, but there are also measurable amplitudes at the harmonics, which could be used for real exploration. As is known, there exist differences between the transmitted signal filtered by the earth and the ideal waveform. Fortunately, the earth does not change the frequency components in the signal, but only the amplitude and phase of the frequency. Therefore, the signal after the ground filtering and the ideal waveform is still very similar in frequency spectrum, as shown in Fig. 6. The low frequency part in Type 7-2 signal maintains the characteristics very well, while the high frequency part is affected to a certain extent.

Since the filtering characteristics under different ground and hardware conditions are not the same, we may take the 2^n sequence pseudo-random ideal signal in Type 7 as an example to discuss the principle of harmonic energy distribution and find potential effective frequencies. Then, a real signal processing example in the field

is shown to illustrate the specific process of effective components extraction in practical applications.

Figure 7 shows the waveform and spectrum of 2^n sequence pseudo-random ideal signal in Type 7-2. The energy distribution of the odd harmonics is significantly different from the periodic square wave. There is no linear relationship between harmonic energy and its order. The corresponding amplitudes of 9, 17 and 21 Hz are all greater than 15 A, while the amplitude of 3 Hz is only 9.87 A.

As shown in Fig. 8, with odd harmonics of 2 Hz, the corresponding current of 18 Hz is 12.91 A, that of 34 Hz is 13.41 A, while the amplitude of 6 Hz is only 9.878 A.

The harmonic amplitude in the 2^n sequence pseudo-random signal is not linearly related to the harmonic order. And the order of the harmonics is no longer applicable as a parameter to predict the amplitude of harmonics.

However, many harmonics have considerable amplitudes and potential exploration capabilities. Extraction of effective components of the 2^n sequence pseudo-random signal cannot focus on these main frequencies or some fixed harmonic frequencies only. Effectiveness screening should be performed on all frequencies according to the signal-to-noise ratio (SNR) in the signal to obtain

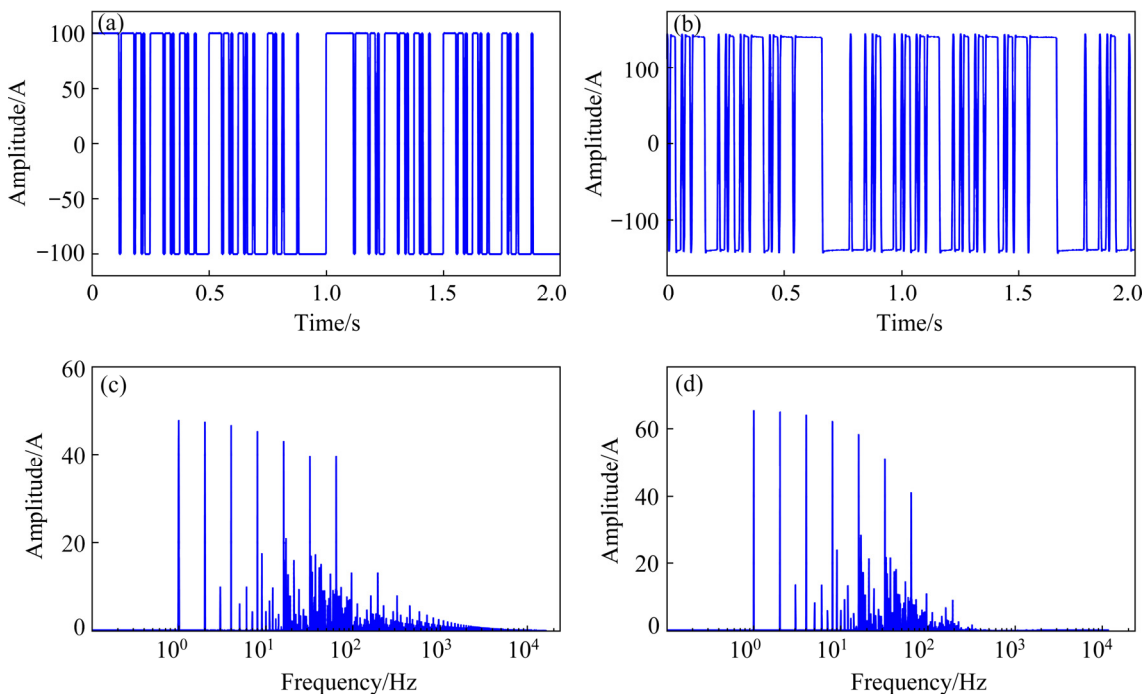


Fig. 6 Ideal waveform (a) and spectrum (c), and real transmitted waveform (b) and spectrum (d) of 2^n sequence pseudo-random signal in Type 7-2

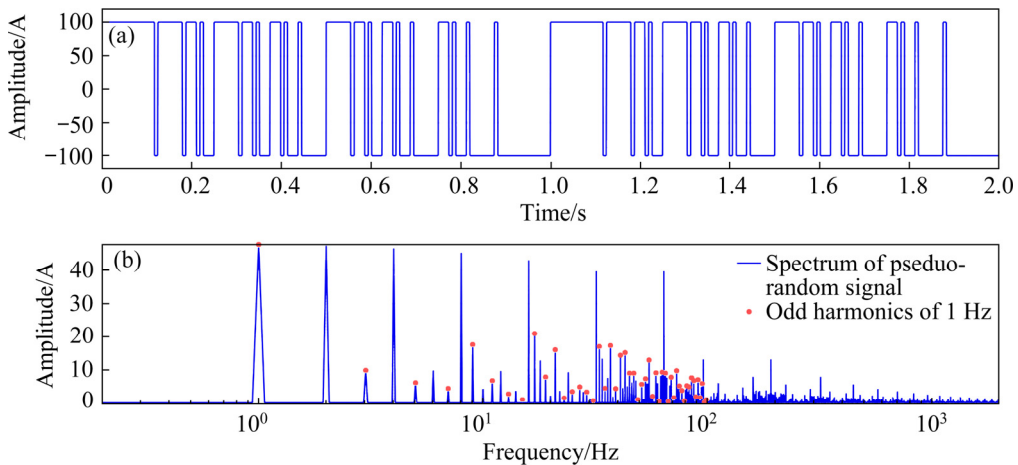


Fig. 7 Waveform (a) and spectrum (b) of WFEM signal in Type 7-2 with odd harmonics of 1 Hz

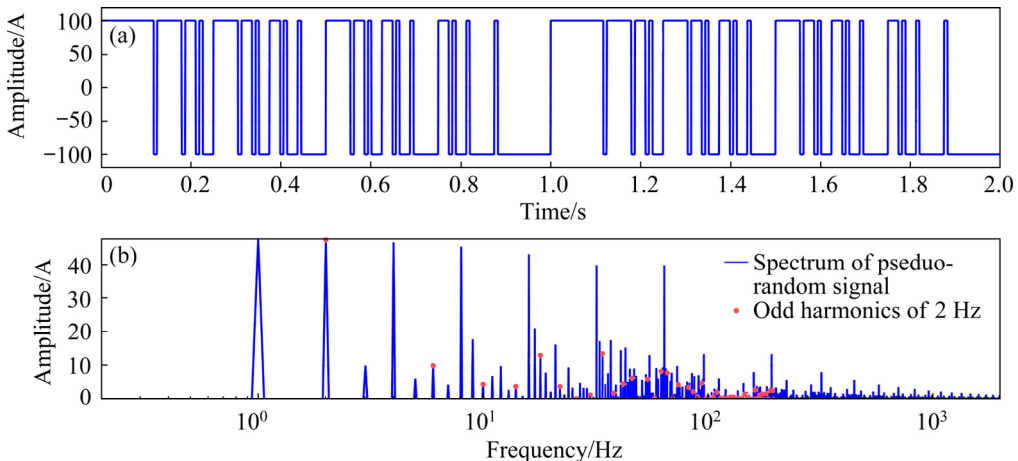


Fig. 8 Waveform (a) and spectrum (b) of WFEM signal in Type 7-2 with odd harmonics of 2 Hz

effective components. In the case of a certain noise, the greater the amplitude is, the higher the signal-to-noise ratio is. Therefore, it is reasonable that the candidate frequencies are first selected according to the amplitude.

We separately screen amplitudes of all main frequencies and harmonics in Type 7 and Type 11 according to different thresholds. Using 25, 8, 5, 2 and 1 A as the threshold to filter the frequencies that meet the amplitude conditions, statistical results are shown in Fig. 9 and Fig. 10, respectively. There are 7, 30, 55, 127 and 251 candidate frequencies extracted from Type 7 signal, while 11, 31, 71, 306 and 673 candidate frequencies extracted from Type 11 signal. Threshold statistics results are listed in Table 1. The number of frequencies above 2 A and 1 A in Type 11 is 2.4 times and 2.6 times that of Type 7, respectively. It is shown that there indeed are a lot of harmonic components with large amplitude in the 2ⁿ sequence pseudo-random signal,

which can be used as the candidate frequencies to perform noise interference evaluation to extract effective components.

3.2 Effective components extraction from 2ⁿ sequence pseudo-random simulation signal

Obviously, the potential effective frequencies need to be filtered before being used as not all candidate frequencies meet the SNR requirements for practical application. We have proposed an algorithm based on wavelet decomposition and analytic envelope for artificial source electromagnetic prospecting signals previously [20], by which we can obtain the SNR information for hundreds of frequencies simultaneously. The main feature of this algorithm is to estimate the upper bound of noise interference, rather than the accurate value of noise interference. Based on this method, we could obtain a parameter named noise ratio to indicate noise impact level on different frequencies.

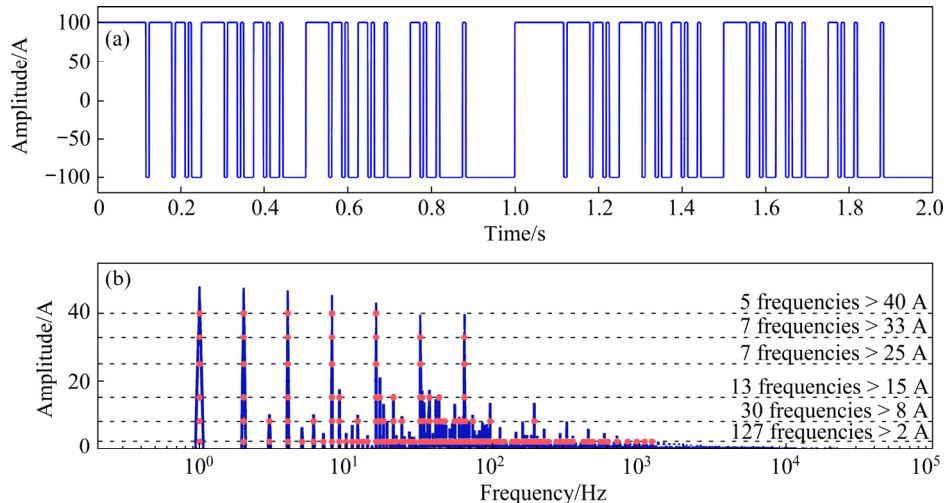


Fig. 9 Waveform of WFEM signal in Type 7-2 (a) and number of frequencies for different amplitude thresholds (b)

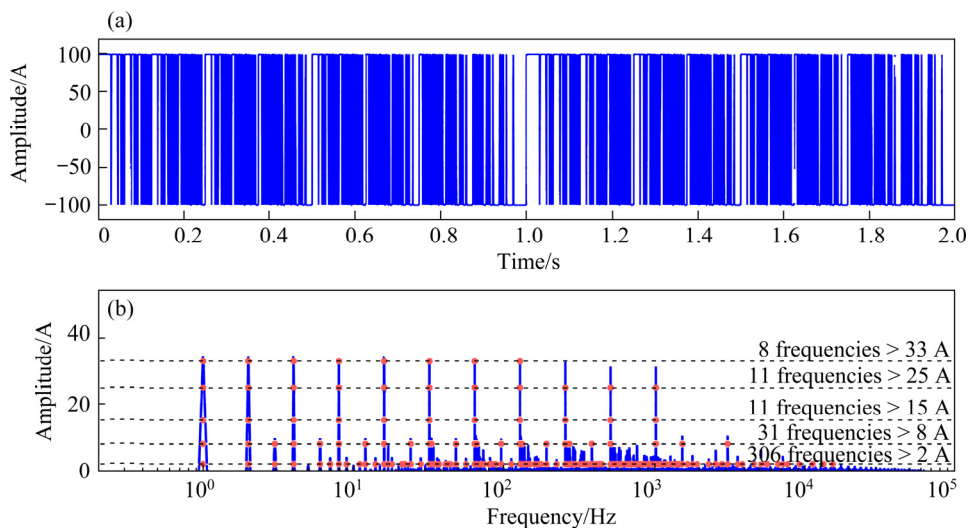


Fig. 10 Waveform of WFEM signal in Type 11 (a) and number of frequencies for different amplitude thresholds (b)

Table 1 Number of screening frequencies for different thresholds of WFEM signal in Type 7 and Type 11

Amplitude threshold/A	Number of frequencies	
	Type 7	Type 11
40	5	0
33	7	8
25	7	11
15	13	11
8	30	31
5	55	71
2	127	306
1	251	673

Real WFEM data are taken to show how to extract those useful frequencies. Observation data are collected in Sichuan Province, China, as an example and obtained through the E-Ex

arrangement. The electric source is used for signal emission, and the electrode is for electric field collection. The waveform and spectrum of the real transmitted signal (current signal) in Type 13 are shown in Fig. 11, with a fundamental frequency of 1 Hz and the highest frequency of 4096 Hz. Affected by long wire inductance and ground filtering, the high-frequency energy of the transmitted signal decays rapidly.

There is a 50 Hz notch filter in the current acquisition equipment, so the frequency spectrum near 50, 100, 150 Hz, and other frequencies is relatively small. By the current threshold screening, as shown in Fig. 12(b), there are 10 frequencies greater than 25 A, 19 frequencies greater than 8 A, and 276 frequencies greater than 1 A in this signal.

For example, taking 1 A as the threshold, we

can obtain 276 candidate frequencies for further processing. By the proposed spectrum envelope algorithm [20], we can obtain the upper bound of noise interference at different frequencies, marked as envelope, for the corresponding received signal, as shown in Fig. 13(a). Then, by dividing this envelope value at those candidate frequencies to the amplitude of corresponding frequency, we can get the noise ratio curve, as shown in Fig. 13(b), for all these 276 candidate frequencies. Taking the value of 2% as the filtering threshold for noise ratio, we can obtain the qualified frequencies. Due to the

influence of industrial noise, the noise ratio near 50 Hz is quite large, and there is no qualified effective component in this range.

Based on the current data, we can also obtain the normalized electric field curve of these qualified frequencies, as shown in Fig. 14, in which the number of qualified frequencies is 75. In other words, by sending only one set of WFEM signal in Type 13, without adding any fieldwork, 75 effective frequencies with high signal-to-noise ratios can be extracted, while in the past only 13 main frequency components were used.

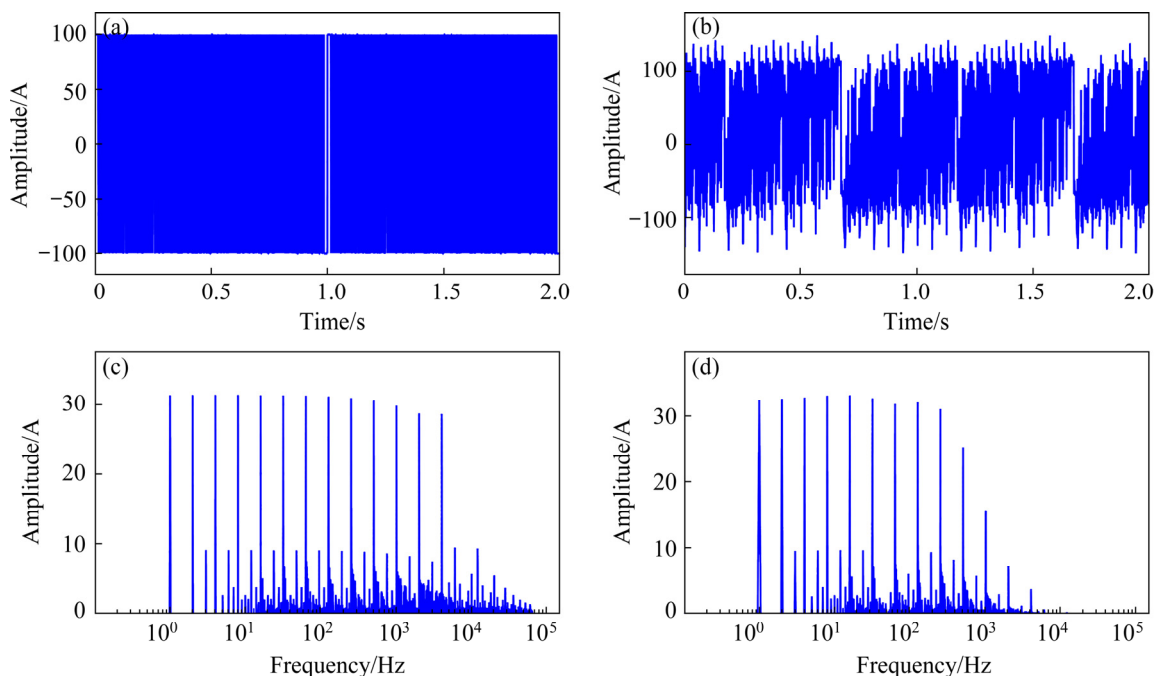


Fig. 11 2^n sequence pseudo-random ideal waveform (a) and spectrum (c), and real transmitted waveform (b) and spectrum (d) in Type 13

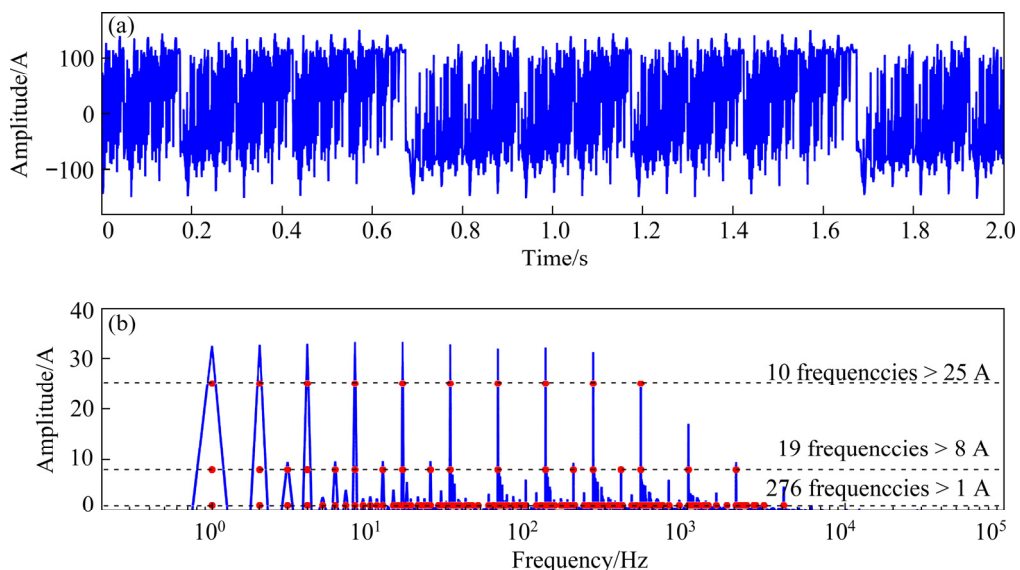


Fig. 12 Waveform of real current signal in Type 13 (a) and number of frequencies for different amplitude thresholds (b)

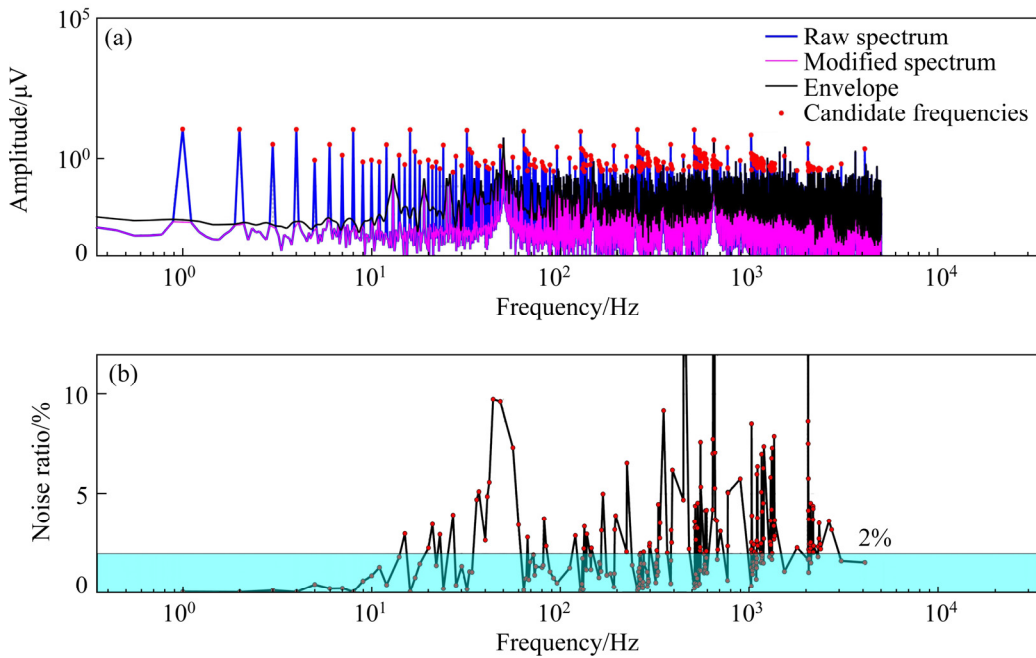


Fig. 13 Spectrum of received WFEM signal in Type 13 (a) and noise ratio for 276 candidate frequencies (b)

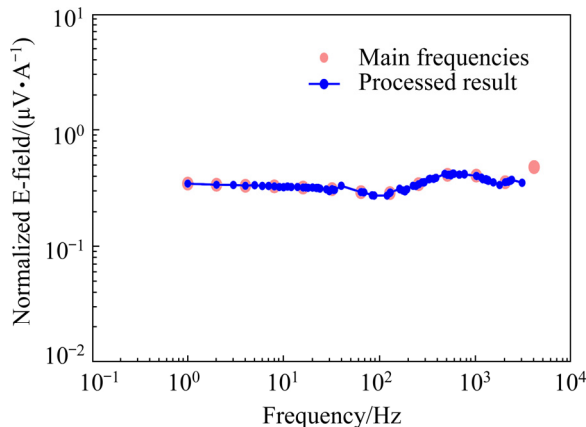


Fig. 14 Normalized E-field of main frequencies only, and processed result

3.3 Calculation method for frequency density

Based on the analysis above, we can see that the distribution of effective harmonics is not uniform, and the absolute number of frequency points cannot well indicate the frequency distribution. Therefore, we propose a new method of frequency density calculation to evaluate the density of effective components in different frequency bands of 2^n sequence pseudo-random signals.

Based on the characteristics of the pseudo-random signal of the 2^n sequence, in the logarithmic coordinates with the base of 2 and the unit length of

1 as the minimum interval unit, the frequency spectrum density is calculated in the interval constructed by 0.5 units on the left and 0.5 units on the right of the corresponding frequency. For example, to calculate the frequency density corresponding to 2^0 Hz, the considered frequency range is $(2^{-0.5} \text{ Hz}, 2^{0.5} \text{ Hz}]$. To more reasonably indicate the effective frequency distribution, a length unit is further divided into 8 equal molecular intervals (other division numbers can be also selected according to the different applications), based on the distribution of the effective components, and the logical number in each subinterval is calculated to replace the absolute number of frequencies in corresponding subinterval. If there is effective frequency in the subinterval, no matter how many, the logical number is set to be 1; if there is no effective frequency in the subinterval, the logical number is set to be 0. The logical number of subintervals are added together to obtain a frequency parameter of unit length, and it is defined as the frequency density to evaluate how much the frequency position corresponds to the effective frequency. With this definition, the minimum frequency density corresponding to any frequency position is 0 and the maximum is 8.

The 2^n sequence 9 frequency wave is taken as an example to illustrate the specific method and

characteristics of the frequency density calculation. The waveform and frequency spectrum are shown in Fig. 15.

If the current amplitude of 20 A is used as the effective frequency screening threshold, 9 effective frequencies can be obtained from the signal, as shown in Fig. 16. For example, the logical number of the sub-interval $(2^{-0.5} \text{ Hz}, 2^{-0.375} \text{ Hz}]$ is 0, the logical number of the sub-interval $(2^{-0.125} \text{ Hz}, 2^0 \text{ Hz}]$ is 1, and the logical numbers of other sub-intervals are all 0, so the spectral parameter of the interval $(2^{-0.5} \text{ Hz}, 2^{0.5} \text{ Hz}]$ is 1, that is, the frequency density is 1. In the same way, the frequency density at the $2^{0.5} \text{ Hz}$ position and the interval spectral parameters of $(2^0 \text{ Hz}, 2^1 \text{ Hz}]$ are calculated, and the frequency

density corresponding to the $2^{0.5} \text{ Hz}$ position is obtained to be 1. By analogy, the spectrum corresponding to different frequencies is obtained based on the spectrum density calculation method, and the spectrum density obtained for this signal 20 A threshold is 1.

If the current amplitude of 5 A is used as the effective frequency threshold, 77 effective frequencies can be obtained from the 2^n sequence pseudo-random signal. The frequency density calculation method of the present invention is used to obtain the frequency density corresponding to different positions to evaluate. Exploration capabilities of different frequency bands are shown in Fig. 17.

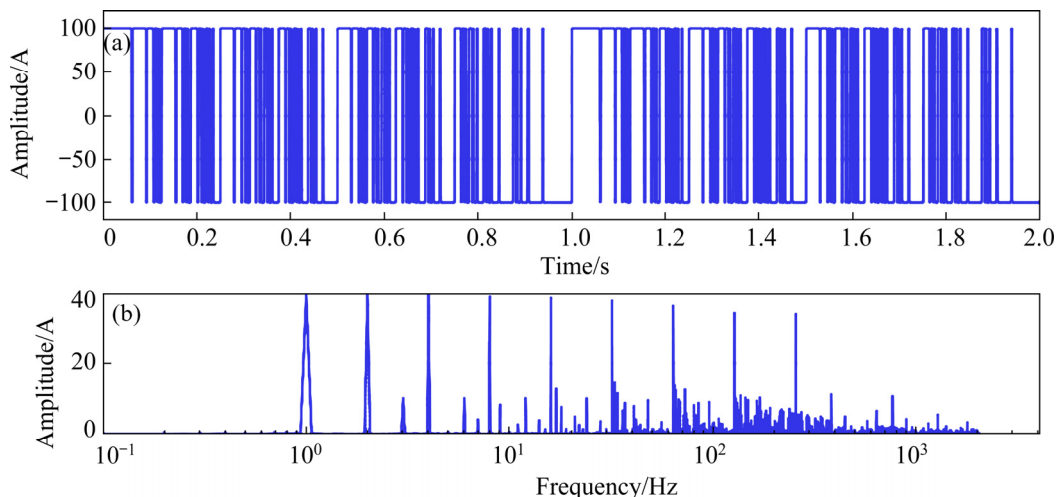


Fig. 15 Waveform of 2^n sequence pseudo-random signal in Type 9 (a) and spectrum of simulation signal (b)

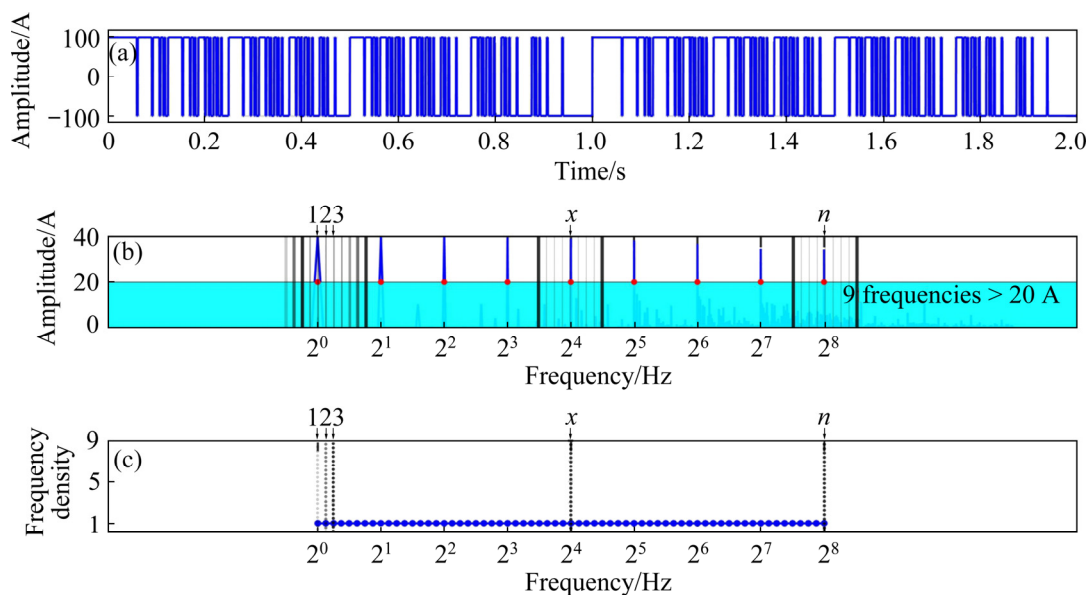


Fig. 16 2^n sequence pseudo-random signal in Type 9 (a), corresponding spectrum of simulation signal (20 A as effective signal threshold) (b), and frequency density curve (c)

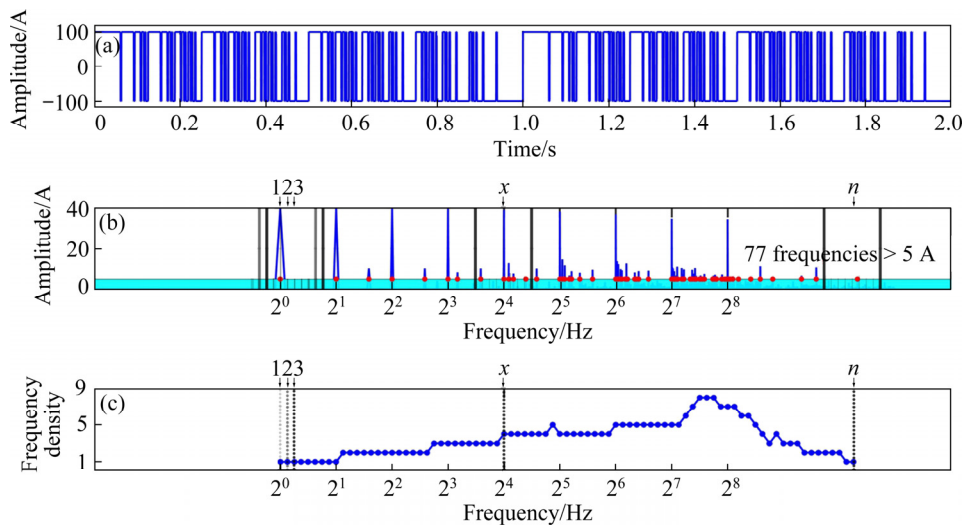


Fig. 17 2^n sequence pseudo-random signal in Type 9 (a), corresponding spectrum of simulation signal (5A as effective signal threshold) (b), and corresponding frequency density curve (c)

This method is operated on the processed result of filed data in Fig. 14. Then, the frequency density is got for this real case, as shown in Fig. 18, which shows the distribution characters of the effective components in different frequency bands.

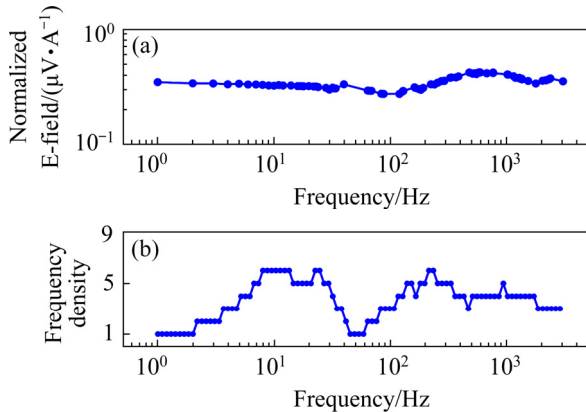


Fig. 18 Normalized E-field of main frequencies of processed result for real filed data in Type 13 (a) and corresponding frequency density curve (b)

4 Conclusions

(1) Based on the average amplitude calculation equation proposed, the average amplitude under any number of main frequencies can be predicted, which provides a reference for the selection of the number of main frequencies of 2^n sequence pseudo-random signal for different exploration tasks.

(2) Besides main frequencies, there exists a lot of effective harmonic components in the 2^n

sequence pseudo-random signal. By screening the corresponding amplitudes of different frequencies of the transmitted signal, the candidate frequencies are obtained. By the spectrum envelope method, the signal-to-noise ratio is calculated at those candidate frequencies in the received data. The qualified frequencies can be extracted as effective components, including main frequencies and harmonics. And the number of effective frequencies is increased without any additional fieldwork.

(3) Compared with the main frequencies, the distribution of effective harmonic components is not logarithmically uniform. Based on the frequency density calculation method proposed, the distribution of effective frequencies can be obtained to indicate the exploration capabilities in different frequency bands.

Acknowledgments

This work was financially supported by the National Key Research and Development Program of China (No. 2019YFC0604902), the National Natural Science Foundation of China (No. 42004056), and the Natural Science Foundation of Shandong Province, China (No. ZR201911010111).

References

[1] STRANGWAY D W, SWIFTC M, HOLMERR C. The application of audio-frequency magnetotellurics (AMT) to

mineral exploration [J]. Geophysics, 1973, 38(6): 1159–1175.

[2] ZONGE K L, HUGHESL J. Controlled source audio-frequency magnetotellurics [M]. 1991: 991.

[3] HE Ji-shan. Controlled source audio-frequency magnetotellurics [M]. Changsha: Central South Industry University Press, 1991. (in Chinese)

[4] CONSTABLE S, SRNKA J. An introduction to marine controlled-source electromagnetic methods for hydrocarbon exploration [J]. Geophysics, 2007, 72(2): WA3–WA12.

[5] BELL M R. Information theory and radar waveform design [J]. IEEE Transactions on Information Theory, 1993, 39(5): 1578–1597.

[6] YANG Y, BLUM R S. Mimo radar waveform design based on mutual information and minimum mean-square error estimation [J]. IEEE Trans Aerosp Electron Syst, 2007, 43(1): 330–343.

[7] STURM C, WIESBECK W. Waveform design and signal processing aspects for fusion of wireless communications and radar sensing [J]. Proceedings of the IEEE, 2011, 99(7): 1236–1259.

[8] AUBRY A, de MAIO A, PIEZZO M, FARINA A. Radar waveform design in a spectrally crowded environment via nonconvex quadratic optimization [J]. IEEE Trans Aerosp Electron Syst, 2014, 50(2): 1138–1152.

[9] MYER D, CONSTABLE C S, KEY K. Broad-band waveforms and robust processing for marine CSEM surveys [J]. Geophysical Journal International, 2011, 184(2): 689–698.

[10] ZIOLKOWSKI A, WRIGHT D, MATTSSON J. Comparison of pseudo-random binary sequence and square-wave transient controlled-source electromagnetic data over the peon gas discovery, Norway [J]. Geophysical Prospecting, 2011, 59(6): 1114–1131.

[11] MITTET R, SCHAUGPETTERSEN T. Shaping optimal transmitter waveforms for marine CSEM surveys [J]. Geophysics, 2008, 73(3): F97–F104.

[12] CONSTABLE S, COX C S. Marine controlled-source electromagnetic sounding: 2. The pegasus experiment [J]. Journal of Geophysical Research: Solid Earth, 1996, 101(B3): 5519–5530.

[13] SRNKA L J, LU X. Logarithmic spectrum transmitter waveform for controlled-source electromagnetic surveying [P]. US Patent 7539279. 2009–05–26.

[14] HE Ji-shan, LIU Jian-xin. Pseudo-random multi-frequency phase method and its application [J]. The Chinese Journal of Nonferrous Metals, 2002, 12(2): 374–376. (in Chinese)

[15] HE Ji-shan. Closed addition in a three-element set and 2ⁿ sequence pseudo-random signal coding [J]. Journal Central South University (Science and Technology), 2010, 41(2): 632–637. (in Chinese)

[16] HE Ji-shan. Wide field electromagnetic method and pseudo random signal method [M]. Beijing: Higher Education Press, 2010. (in Chinese)

[17] HE Ji-shan, YANG Yang, LI Di-quan, WENG Jing-bo. Method and system for generating high-order pseudo-random electromagnetic prospecting signal [P]. CN Patent 2020103447332. 2020–08–11.

[18] HE Ji-shan, LI Fang-shu, WANG Yong-bing. Method and system for hybrid coding of pseudo-random signal [P]. CN Patent 2018113093182. 2019–04–05.

[19] BRACEWELL R N. The Fourier transform & its applications [M]. WCB/McGraw Hill, 2000.

[20] YANG Yang, HE Ji-shan, LI Di-quan. A noise evaluation method for CSEM in the frequency-domain based on wavelet transform and analytic envelope [J]. Chinese Journal of Geophysics, 2018, 61(1): 344–357. (in Chinese)

2ⁿ序列伪随机信号中的能量分布与有效成分分析

杨 洋¹, 何继善^{2,3}, 李帝铨³

1. 山东大学 岩土与结构工程研究中心, 济南 250061;
2. 香港中文大学(深圳) 城市地下空间及能源研究院, 深圳 518172;
3. 中南大学 地球科学与信息物理学院, 长沙 410083

摘要: 为获取2ⁿ序列伪随机信号中的有效谐波成分, 提出一种提取有效成分的方法。从能量守恒定律出发, 首先提出一种主频平均幅值的估计方法, 以此根据不同的勘探任务选择合适的发送波形。针对实际发送电流, 通过阈值筛选获取潜在有效频率; 对接收数据在频率域进行频谱包络, 获取潜在有效频率所对应噪声评价数; 基于该噪声评价数, 通过给定阈值筛选获得勘探信号中的有效成分。针对有效成分在频率域分布特点, 提出一种新的频率密度计算方法, 以评价不同频段的频率疏密程度。在四川某地, 通过应用所提出方法, 成功从13频波勘探数据中获取75个有效频率, 既包含主频, 又包含谐波成分。通过提取2ⁿ序列伪随机信号中的有效谐波成分, 能够在不增加任何野外工作量的情况下, 大大增加有效频率数目。

关键词: 电磁勘探; 2ⁿ序列伪随机信号; 能量守恒; 谐波提取; 频率密度